Electronic Supplementary Information (ESI)

Controllable Selenium Vacancy Engineering in Basal Planes of WSe_2 Mechanically Exfoliated Monolayer Nanosheets for Efficient Electrocatalytic Hydrogen Evolution

Ying Sun, Xuewei Zhang, Baoguang Mao and Minhua Cao*

Key Laboratory of Cluster Science, Ministry of Education of China, Beijing Key Laboratory of Photoelectronic/Electrophotonic Conversion Materials, School of Chemistry and Chemical Engineering, Beijing Institute of Technology, Beijing 100081, P. R. China. E-mail: *caomh@bit.edu.cn*

1. Experimental Section

1.1 Preparation of WSe_2 MLNSs

Typically, 1 g of commercial WSe_2 powder was first dispersed in 10 mL of N-methyl-2-pyrrolidone (NMP) in a mortar. After grinding for 30 min, the resultant dispersion was added into 90 mL of NMP in serum bottle and kept sonication for 10 h to exfoliate WSe_2 powder by sonicator (KQ5200DB) with an output power of 200 W. Then the top 2/3 of the dispersion was decanted into flask and kept vigorous stirring for 12 h at 150 °C. Afterwards, the resulting suspension was centrifuged for 20 min at 9000 rpm to separate the centrifugate and supernatant. Then the ethanol was added into the centrifugate and the resulting suspension was centrifuged for 5 min at 3000 rpm. The resultant supernatant was dried by vacuum freeze dryer and finally WSe_2 MLNSs were collected. Note that the sonication and the heating reflux of WSe_2 should be operated in an Ar gas atmosphere to avoid its oxidation. Subsequently, the WSe_2 MLNSs were annealed in an Ar/H_2 atmosphere (Ar: H_2 = 95: 5, in volume) at 700 ^oC and 900 ^oC for 90 min at a heating rate of 20 ^oC min^{-1} to obtain WSe_2 MLNSs-700 and WSe_2 MLNSs-900.

1.2 Structural characterizations

The composition and purity of the final samples were characterized using powder X-ray diffraction (XRD) with Cu Kα (λ = 1.54178 Å) incident radiation (Shimadzu XRD-6000). The corresponding scanning range and step were recorded from 10 to 80° (2θ) and 10 ° min^{-1}, respectively. The morphology of the resulting samples was investigated by transmission electron microscopy (TEM) (H-8100, with the accelerating voltage of 200 kV), field emission scanning electron microscopy (FE-SEM) (Hitachi S-4800), and atomic force microscopic (AFM) (Tapping–mode AFM, Agilent SPM 5500). Raman spectra were collected on an Invia Raman spectrometer, using an excitation laser of 514.5 nm. X-ray photoelectron spectra (XPS) were used to characterize the surface composition of the sample by using an ESCALAB 250

spectrometer (Perkin-Elmer). The X-ray absorption near edge structure (XANES) measurements were undertaken at Beamlines 1W1B at Beijing Synchrotron Radiation Facility (BSRF) using transmission and fluorescence modes.

1.3 Electrochemical measurements

Electrochemical measurements were performed in a three-electrode system at an electrochemical station (CHI660D). The three-electrode configuration was adopted for polarization and electrolysis measurements, where a Ag/AgCl (KCl saturated) electrode, a graphite rod and a glassy carbon (GC) electrode modified by WSe_2-based catalyst were used as the reference electrode, the counter electrode and the working electrode, respectively. Linear sweep voltammetry with a scan rate of 10 mV s^{-1} was conducted in 0.5 M H_2SO_4 and 1 M KOH solution. For a Tafel plot, the linear portion is fit to the Tafel equation. Electrochemical impedance spectroscopy (EIS) was performed by applying a sine wave with amplitude of 5 mV over the frequency range from 100 kHz to 0.01 Hz at -0.3 V in 0.5 M H_2SO_4. All data have been corrected for a small ohmic drop based on impedance spectroscopy. All the potentials were calibrated to a reversible hydrogen electrode (RHE). The WSe_2-based electrodes were prepared as follows: (1) 2 mg of WSe_2 was dispersed in 1 mL of ethanol/water mixture (ethanol:water = 4.5: 5.5, in volume) by sonicating for 30 min to form a homogeneous solution; (2) 30 μL portion of the resulting solution was dropcast onto a GC electrode with 3 mm diameter by a microliter syringe and dried at room temperature and the catalyst loading mass on electrode is 0.85 mg/cm^2. (4) 10 μL of Nafion solution (5 wt.%) was dropcast onto the GC electrode and dried at room temperature. The commercial Pt/C electrode was prepared by the same method with the WSe_2-based electrodes and the loading mass of the Pt/C catalyst on electrode is also 0.85 mg/cm^2.

2. Theoretical calculation methods

All calculations in this work were performed using Vienna ab initio simulation package (VASP). Electron exchange and correlation were treated using the Perdew-Burke-Ernzerhof (PBE) parametrization of the generalized-gradient approximation. A

plane-wave cutoff of 500 eV was used, and a Monkhorst-Pack 4×4×1-point grid was used to sample the Brillouin zone, i.e. 4 k-points in the x and y-direction, and 1 k-points in the z-direction, respectively. Periodic boundary conditions were used in all directions and 11 Å of vacuum was used in the z-direction to separate the slabs, which are 4 Se atoms × 4 W atoms in size. The hydrogen absorption free energies were determined in the same way as in previous studies. For the structural relaxations, the convergence criteria of 0.02 eV $Å^{-1}$ were used for the maximum force.

The calculation of hydrogen adsorption free energy: The hydrogen adsorption free energies, ΔG_H, were determined in the same way as in previous studies.[1-3] The adsorption energy is defined as:

$$\Delta E_H = E(WSe_2+H) - E(WSe_2) - 1/2\ E(H_2) \qquad (1)$$

where (WSe_2+H) refers to hydrogen adsorbed on the WSe_2 surface, (WSe_2) refers to a clean WSe_2 surface, and H_2 refers to gas phase hydrogen molecule. The hydrogen adsorption free energy was calculated at zero potential and pH = 0 as:

$$\Delta G_H = \Delta E_H + \Delta E_{ZPE} - T\Delta S \qquad (2)$$

where ΔE_H is the hydrogen adsorption energy, ΔE_{ZPE} is the difference in zero point energy, T is the temperature (300 K) and ΔS is the difference in entropy between H that is adsorbed and in the gas phase, at 101325 Pa. A normal mode analysis was used to determine the vibrational frequencies of the adsorbed species, which were used to determine the zero point energy correction and the entropy. The adsorption is too strong if ΔG_H is very negative or too weak if ΔG_H is very positive.

3. Figures and captions

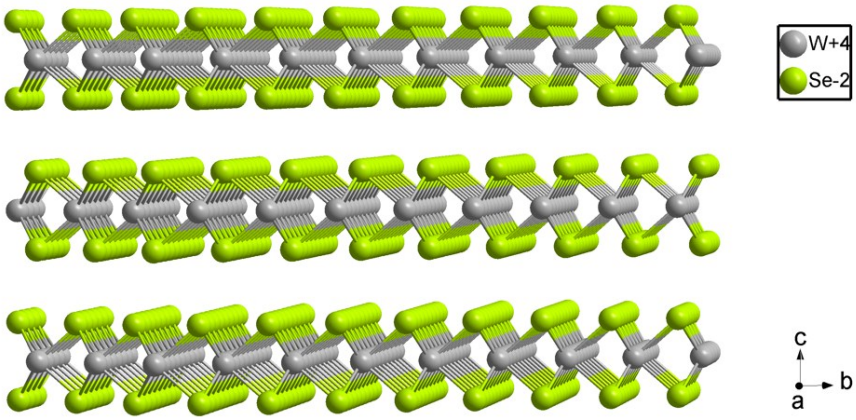

Fig. S1 The crystal structure of WSe_2.

WSe_2 has a lamellar structure, in which the individual Se-W-Se layers weakly interact with each other by Van der Waals force.

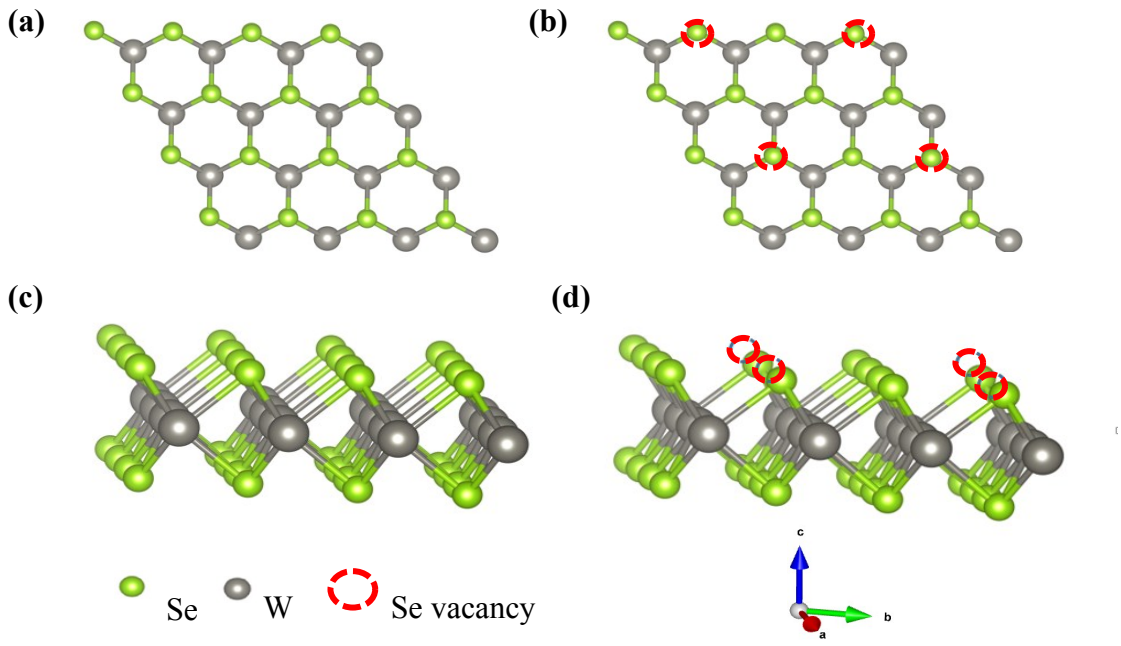

Fig. S2 Computational unit cell of WSe_2. Top view (upper panel) of the atomic structures of the WSe_2 basal plane with 0% (a) and 12.5% Se-vacancies (b). Side view (lower panel) of the atomic structures of the WSe_2 basal plane with 0% (c) and 12.5% Se-vacancies (d).

Each unit cell consists of 16 W atoms and 32 Se atoms on the surface. Assuming that Se-vacancies are only formed on the surface (top side of the monolayer), in this unit cell size, the concentration of Se-vacancies with the increment of 3.12% is possible, where the 3.12% is defined as the total number of the Se-vacancies divided by the total number of Se atoms in the pristine basal plane. All subsequent Se-vacancies from the first one were spaced out as far as possible from existing Se-vacancies. For the range of Se-vacancies considered in this work, we observe no noticeable rearrangement in the geometry.

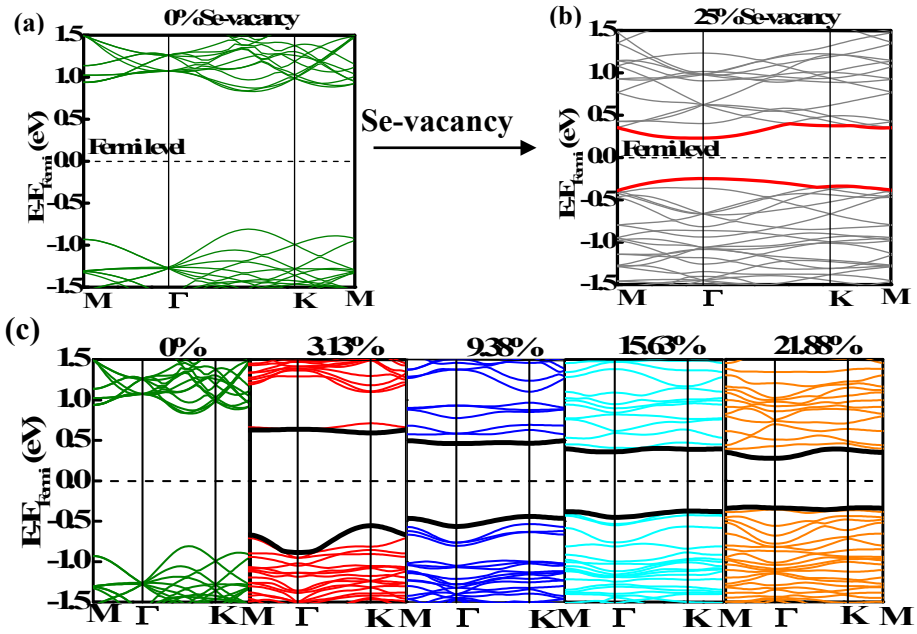

Fig. S3 Band structure of WSe_2 MLNSs with 0% (a) and 25% Se-vacancies (b). (c) Tuning the band structure by increasing Se-vacancy concentration. The bands nearest to the Fermi level are highlighted in black.

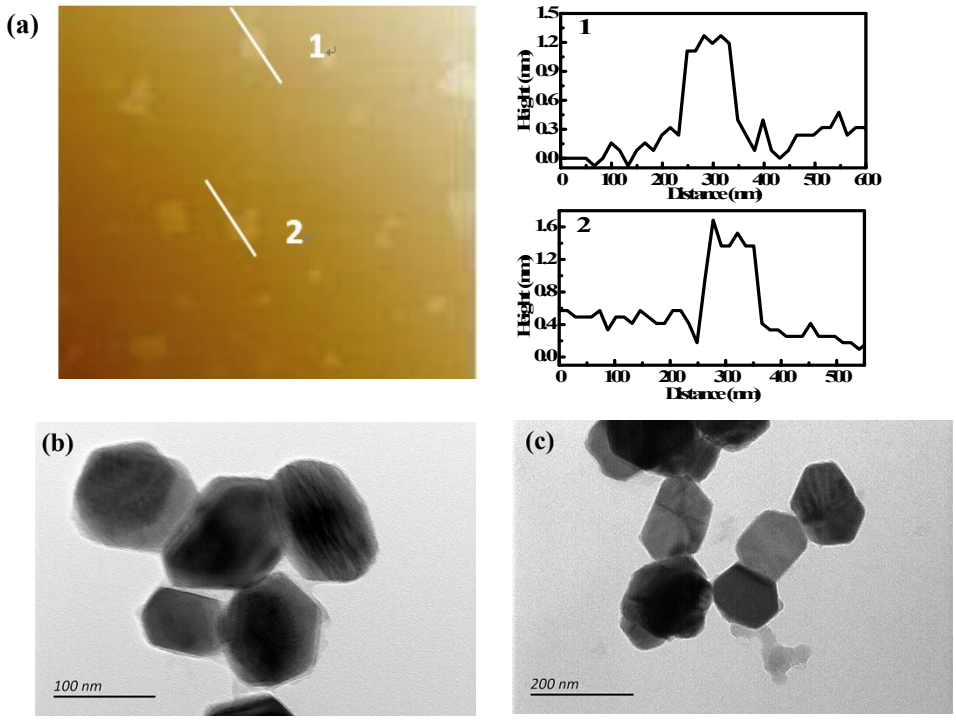

Fig. S4 (a) AFM image and height profiles of WSe_2 MLNSs. TEM images of WSe_2 MLNSs-700 (b) and WSe_2 MLNSs-900 (c).

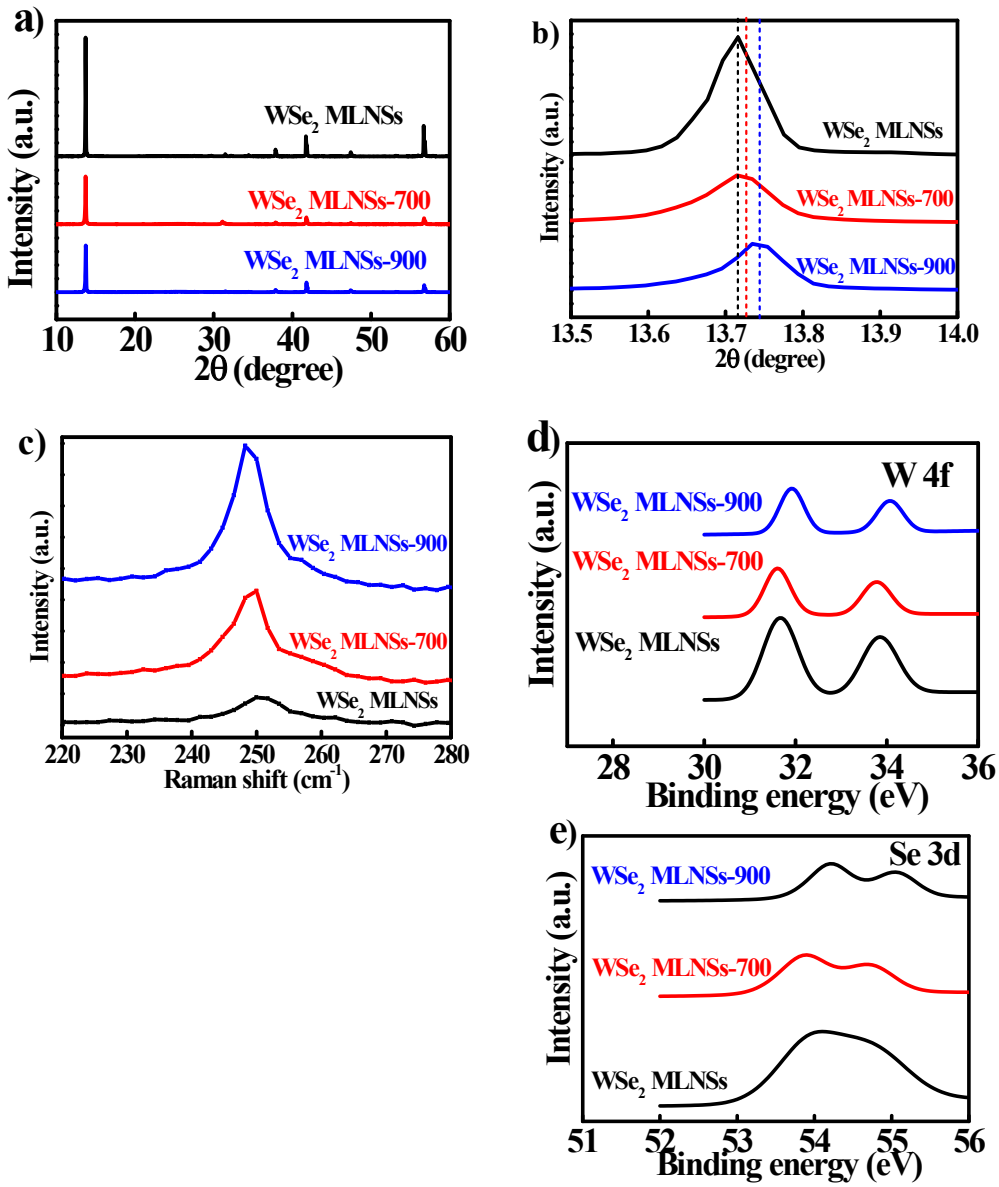

Fig. S5. (a) wide-angle and (b) narrow-angle XRD patterns of WSe_2 MLNSs, WSe_2 MLNSs-700 and WSe_2 MLNSs-900. (c) Raman spectra of WSe_2 MLNSs, WSe_2MLNSs-700 and WSe_2 MLNSs-900. High-resolution XPS spectra of W 4f (d) and Se 3d (e) of WSe_2 MLNSs, WSe_2 MLNSs-700 and WSe_2 MLNSs-900.

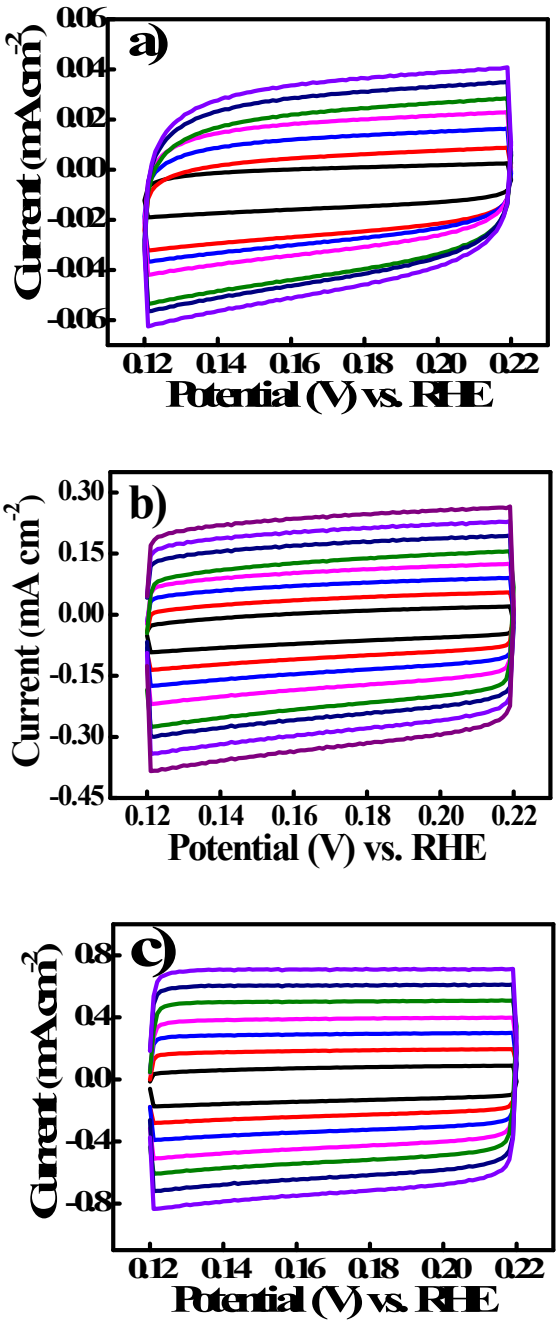

Fig. S6 Cyclic voltammograms of (a) WSe_2 MLNSs, (b) WSe_2 MLNSs-700 and (c) WSe_2 MLNSs-900 electrodes at various scan rates (20-140 mV s^{-1}).

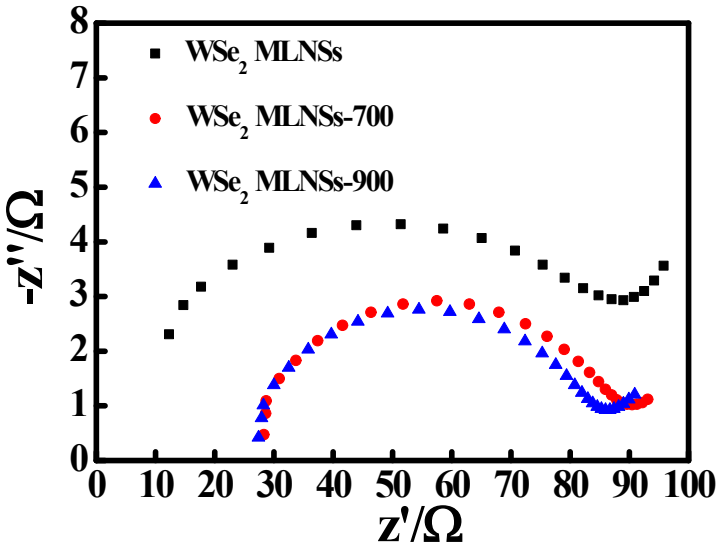

Fig. S7 ESI spectra of WSe_2 MLNSs, WSe_2 MLNSs-700 and WSe_2 MLNSs-900.

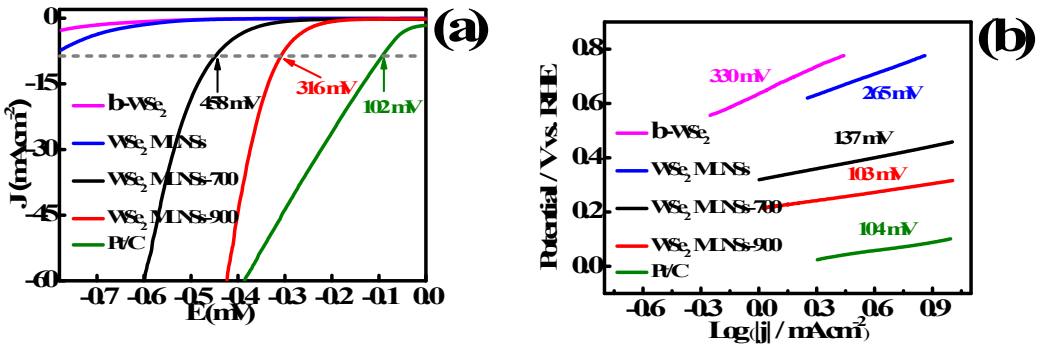

Fig. S8 (a) HER polarization plots of all samples in 1.0 M KOH. (b) Tafel plots obtained from the polarization curves in (a).

Table S1. The composition of the samples estimated from the XPS measurements.

Sample	WSe_2MLNSs	WSe_2MLNSs-700	WSe_2MLNSs-900
x in WSe_{2-x}	0	0.1	0.13

Table S2. Structural parameters around W atoms extracted from XAFS curve-fitting for WSe_2 MLNSs, WSe_2 MLNSs-700 and WSe_2 MLNSs-900, respectively.

Sample	Path	R (Å)	N	σ^2 (10^{-3} Å^2)	ΔE_0 (eV)
WSe_2 MLNSs	W-Se	2.529	6.00	2.469	7.7
WSe_2 MLNSs-700	W-Se	2.528	5.50	2.503	7.6
WSe_2 MLNSs-900	W-Se	2.527	5.40	2.552	7.7

Table S3. Electrocatalytic performance of the three different catalysts.

Catalyst	Onset potential (mV)	η@ j=10 mA/cm^2 (mV)	Tafel slope(mV/ decade)	C_{dl} (mF/ cm^2)	j_0 (×10^{-6} A/ cm^2)
WSe_2 MLNSs	200	563	95	0.56	0.38
WSe_2 MLNSs-700	151	318	90	3.53	3.17
WSe_2 MLNSs-900	125	245	76	10.21	6.14

Table S4. The onset overpotential, overpotential at 10 mA cm^{-2} and Tafel slope of various electrocatalysts for HER.

Catalysts	Onset overpotential (mV)	Overpotential at 10 mA cm^{-2} (mV)	Tafel slope (mV/decade)	Refs.
$WS_{2(1-x)}$ Se_{2x} NTs on CFP	—	~300	105	1b
$MoSe_{2-x}$ NSs	170	~290	98	2a
1T-MoS_2 NSs	100	~220	40	3c
WSe_2 nanofilm on CFP	—	300	77	4b
WS_2 QDs anchored in WS_2 NSs	180	~350	75	7a
MoS_2 QDs	160	~320	58	10
WSe_2 MLNSs-900	125	245	76	This work

NTs: nanotubes; CFP: carbon fiber paper; NSs: nanosheets; QDs: quantum dots.

References

1 H. Li, C. Tsai, A. L. Koh, L. L. Cai, A. W. Contryman, A. H. Fragapane, J. H. Zhao, H. S. Han, H. C. Manoharan, F. Abild-Pedersen, J. K. Norskov, X. L. Zheng, *Nat. Mater.*, 2016, **15**, 48.

2 C. Tsai, K. Chan, F. Abild-Pedersen, J. K. Norskov, *Phys. Chem. Chem. Phys.,* 2014, **16**, 13156.

3 C. Tsai, K. Chan, J. K. Nørskov, F. Abild-Pedersen, *Surf. Sci.,* 2015, **640**, 133.